Molecular Physics
Vol. 00, No. 00, Month 200x, 1–17

RESEARCH ARTICLE

Structure factors in a two-dimensional binary colloidal hard sphere system

Alice L. Thorneywork[a,b], Simon K. Schnyder[c], Dirk G. A. L. Aarts[a], Jürgen Horbach[e], Roland Roth[d] and Roel P. A. Dullens[a]

[a] *Department of Chemistry, Physical and Theoretical Chemistry Laboratory, University of Oxford, South Parks Road, Oxford OX1 3QZ, United Kingdom*; [b] *Cavendish Laboratory, University of Cambridge, Cambridge CB3 0HE, United Kingdom*; [c] *Fukui Institute for Fundamental Chemistry, Kyoto University, Kyoto 606-8103, Japan*; [d] *Institut für Theoretische Physik, Universität Tübingen, Auf der Morgenstelle 14, 72076 Tübingen, Germany*; [e] *Institut für Theoretische Physik II, Heinrich-Heine Universität Düsseldorf, Universitätsstrasse 1, 40225 Düsseldorf, Germany*

(*Received 00 Month 200x; final version received 00 Month 200x*)

Hard disks are the simplest interacting many-body model system with a purely repulsive potential in two dimensions. Here, we present a comprehensive set of measurements of the static structure factors for quasi two-dimensional monodisperse fluids and two different binary colloidal hard sphere mixtures: a small size ratio ($\gamma = 1.45$) system with a negligibly small negative non-additivity and a large size ratio ($\gamma = 2.19$) system with a significantly larger non-additivity. We compare the experimental results for the monodisperse and small size ratio systems to those calculated using a density functional theory for additive mixtures. Furthermore, we determine the zero wavevector limits of the static structure factors for the monodisperse and binary hard sphere fluids directly from an analysis of number and concentration fluctuations. For the monodisperse case, this leads to the isothermal compressibility, which agrees very well with density functional theory, and is consistent with the scaled particle theory equation of state for hard disks. For the binary fluids, the partial static structure factors are used to calculate the Bhatia–Thornton structure factors, and we find qualitative agreement with density functional theory for the small size ratio mixture. Finaly, the zero-wavevector limits of the Bhatia–Thornton structure factors are determined, which are directly related to the thermodynamic factor, the dilatation factor and the isothermal compressibility.

1. Introduction

Most materials of practical interest consist of more than a single component, yet elucidating the physical behaviour of multicomponent systems is extremely challenging. Nevertheless, these systems, which include metallic alloys [1–6], polymer blends [7–9] and glasses [10–13] are important for a range of applications, making this detailed understanding crucial for the development of more sophisticated materials. Here, a key difficulty is that multicomponent systems often display markedly different properties from those of their pure components, with precise details of the interactions and cross-correlations between species leading to a range of subtle effects [14–16]. The simplest multicomponent system to consider is a binary mixture, i.e. a system consisting of only two components. However, even these 'simple' binary mixtures already display a rich range of physical behaviour beyond that seen in a single component system [17–23]. This includes different phase transitions,

*Corresponding author. Email: roel.dullens@chem.ox.ac.uk

ISSN: 0040-5167 print/ISSN 1754-2278 online
© 200x Taylor & Francis
DOI: 10.1080/0040516YYxxxxxxxx
http://www.informaworld.com

such as fluid-solid phase separation [24–26], and glass formation [11–13, 27, 28], with binary solids forming alloys or glasses depending upon the structural order of the individual particles [29–31]. Even in a single fluid phase the correlation functions display a much richer behaviour than a one-component system, as the unique wavelength of oscillation in a mixture can either be set by the size of the smaller or the large particles of a mixture. The transition from one to the other length-scale is called structural crossover [32, 33], which can be observed not only in bulk correlation functions but also in several inhomogeneous distributions. Structural crossover has been observed experimentally in binary colloidal fluids [34, 35] and ionic liquid–solvent mixtures [36]

The simplest interacting binary system is that of a mixture of large and small hard spheres with diameters $\sigma_{l,s}$. The behaviour of binary hard spheres is governed by the total packing fraction, $\phi_t = \phi_l + \phi_s$, with $\phi_{l,s}$ the packing fractions of the large and small hard spheres, the composition $q = \phi_l/\phi_t$ and the size ratio $\gamma = \sigma_l/\sigma_s$. However, for binary hard sphere mixtures at relatively large size ratios, non-additivity effects can give rise to complex behaviour, as is evident from the vast amount of theoretical and simulation studies [18–21, 23, 37, 38]. Experimentally, hard sphere model systems can be realised using colloids [39], and previous work on three-dimensional binary colloidal hard sphere system has included studies of phase separation [24], crystallisation [29] and glass formation [13]. In two dimensions (2D), the situation is markedly different with the phase behaviour of monodisperse hard disks only recently having been established in simulations [40–42] and in experiments on 2D colloidal hard spheres [43, 44]. We note here that in these experiments the colloidal hard spheres are confined to a monolayer and can – in the plane of the centres of the spheres – be considered as an excellent experimental hard disk system [45–47]. For hard disks in particular, the increased complexity in the behaviour of binary mixtures is nicely illustrated by the fact that the melting behaviour of monodisperse hard disks qualitatively changes with the addition of a second component [16].

While a comprehensive study of the radial distribution functions in both single component and binary hard disk systems was reported in [45], its counterpart in Fourier space, the (partial) static structure factor $S_{ij}(k)$,

$$S_{ij}(k) = \frac{1}{N}\left\langle \sum_{\nu=1}^{N_i}\sum_{\mu=1}^{N_j} \exp\left[i\mathbf{k}\cdot(\mathbf{r}_\nu - \mathbf{r}_\mu)\right]\right\rangle, \tag{1}$$

has received much less attention, despite the fact that there is a direct link between the zero-wavevector ($k \to 0$) limit of the static structure factor and thermodynamic quantities. In Eq. (1) i, j may either represent the small or large particles, $\mathbf{r}_{\nu,\mu}$ is the position of particle ν of species i or μ of species j, $k = |\mathbf{k}|$ is the wavevector and N is the number of particles. For monodisperse systems, for example, this link directly leads to the isothermal compressibility, χ_T, as

$$S(k \to 0) = \rho k_B T \chi_T, \tag{2}$$

where ρ is the number density, k_B the Boltzmann constant and T the temperature. As will be discussed later, the isothermal compressibility quantifies macroscopic fluctuations in the number of particles. For binary systems determining the isothermal compressibility is much more challenging. In fact, a full description of a binary mixture requires the knowledge of multiple thermodynamic quantities that follow from specific linear combination of the partial static structure factors. These linear combinations are known as the Bhatia–Thornton structure factors and are defined

as [1–3]

$$S_{nn} = S_{ll} + S_{ss} + 2S_{ls}, \tag{3}$$

$$S_{cc} = c_s^2 S_{ll} + c_l^2 S_{ss} - 2c_l c_s S_{ls}, \tag{4}$$

$$S_{nc} = c_s S_{ll} - c_l S_{ss} + (c_s - c_l) S_{ls}, \tag{5}$$

with $c_i = N_i/N$ $(i = l, s)$ the concentration of component i and N_i the number of large or small particles. Whilst the partial static structure factors describe correlations between like or unlike particles, the Bhatia–Thornton structure factors instead consider number-number (nn), concentration-concentration (cc) and number-concentration (nc) correlations.

In the $k \to 0$ limit, these Bhatia–Thornton structure factors are related to the thermodynamic quantities of the binary mixture as [1–3]

$$S_{nn}(0) = \rho k_\mathrm{B} T \chi_T + \delta^2 S_{cc}(0), \tag{6}$$

$$S_{cc}(0) = c_l c_s / \Phi, \tag{7}$$

$$S_{nc}(0) = -\delta S_{cc}(0). \tag{8}$$

Here, Φ is the thermodynamic factor, χ_T the isothermal compressibility of the mixture and $\delta = \rho(v_l - v_s)$ the dilatation factor with $v_{l,s}$ the partial molar volumes. The isothermal compressibility for binary mixtures is analogous to that for single component systems (Eq. (2)), however, as the $k \to 0$ limits of the Bhatia–Thornton structure factors are all interdependent, χ_T for mixtures cannot be obtained from the limit of a single static structure factor. As such, the determination of χ_T for mixtures requires that all the limits in Eqs. (6) – (8) are obtained to a high degree of accuracy. The thermodynamic factor Φ, which follows from $S_{cc}(0)$ and is directly related to the second derivative of the molar Gibbs free energy $\partial^2 g/\partial c_l \partial c_s$ [48], plays a key role in transport processes like mutual diffusion or interdiffusion [6] as the variation of the thermodynamic factor is directly linked to the nature of the concentration fluctuations. Importantly, the thermodynamic factor accounts for the tendency of concentration fluctuations to relax over large length scales and these concentration fluctuations are indicative of the overall stability of the mixture [6]. For example, the long range concentration fluctuations characteristic of a phase separating system close to the critical point, thus lead to a large $S_{cc}(0)$ and a correspondingly small Φ [22]. For binary systems that tend to order rather than phase separate, the opposite behaviour is seen and the thermodynamic factor becomes large [6]. Once Φ is known, the dilatation factor, δ, which describes the relationship between system size and composition [1–3], follows from $S_{nc}(0)$ and the compressibility χ_T then results from $S_{nn}(0)$.

In this article, we present a detailed and comprehensive analysis of static structure factors for quasi-two dimensional monodisperse and binary colloidal hard spheres and compare these to those calculated using density functional theory. We determine the $k \to 0$ limits of the structure factors from the analysis of the number and concentration fluctuations. For the compressibility of monodisperse systems we find good agreement between results of the fluctuation analysis, density functional theory and the previously determined equation of state [43, 45]. We next consider the Bhatia–Thornton structure factors as a function of the total packing fraction for binary systems at two different size ratios. We again find that an analysis of the relevant fluctuations provides a good estimate for the $S(k \to 0)$ limit for these mixtures, allowing us to obtain the key thermodynamic quantities,

such as the variation of the isothermal compressibility, the dilatation factor and the thermodynamic factor as a function of the total packing fraction.

2. Density Functional Theory

Classical density functional theory (DFT) is a versatile tool for the inhomogeneous structure and thermodynamics of (classical) fluids and solids [49]. One can proof that a functional of the grand potential Ω exists that takes its minimum for the equilibrium density distribution, where it reduces to the grand potential of the system [49]. The functional for a mixture takes the form

$$\Omega[\{\rho_i\}] = \mathcal{F}_{id}[\{\rho_i\}] + \mathcal{F}_{ex}[\{\rho_i\}] + \sum_i \int d\mathbf{r}\ \rho_i(\mathbf{r}) \left(V^i_{ext}(\mathbf{r}) - \mu_i\right), \tag{9}$$

where the ideal gas (id) contribution is known exactly. $V^i_{ext}(\mathbf{r})$ and μ_i is the external and the chemical potential of species i, respectively. Beside the aforementioned important property of the functional, that can be shown with mathematical rigor, one has to construct a functional of the intrinsic excess free energy $\mathcal{F}_{ex}[\{\rho_i\}]$, which contains all the information about particle-particle interaction. For most systems of interest, the functional of the excess free energy relies on approximations. For hard particles Rosenfeld [50] introduced fundamental measure theory (FMT) which is in contrast to other theories from the onset a theory, for mixtures. The structure of the intrinsic excess free energy functional is given by [50, 51]

$$\mathcal{F}_{ex}[\rho] = k_B T \int d\mathbf{r}\ \Phi_{FMT}(\{n_\alpha\}), \tag{10}$$

where Φ_{FMT} is the reduced excess free energy density for a mixture of hard spheres in three dimensions or of hard disks in two dimensions. Φ_{FMT} is a function (not a functional) of a set of weighted densities. Note that Φ_{FMT} should not be confused with the thermodynamic factor Φ. For a z–component mixture the weighted densities are given by

$$n_\alpha(\mathbf{r}) = \sum_{i=1}^{z} \int d\mathbf{r}'\ \rho_i(\mathbf{r}')\ \omega_i^\alpha(\mathbf{r}, \mathbf{r}'), \tag{11}$$

which is a convolution of local densities of species i, $\rho_i(\mathbf{r})$, with geometrical weight functions ω_i^α.

In this work we are interested in the theoretical description of binary colloidal hard spheres confined to a monolayer. This is best done by a DFT for hard disks. While for hard spheres in three dimensions there exists a FMT functional that can treat mixtures of non-additive hard spheres [38], in two dimensions only additive mixtures can be treated [52, 53]. Details about the functional and the geometrical weight functions for hard disks are given in Ref. [52].

Here, we present the Ornstein-Zernike route [48] to the static structure factor for a bulk fluid of hard disks from a recent density functional theory (DFT) [52] within the framework of fundamental measure theory (FMT) [50, 51]. The starting point for the one-component fluid is the connection between the static structure factor $S(k)$ and the Fourier transform $c^{(2)}(k)$ of the pair direct correlation function

$c^{(2)}(r)$ [48]

$$S(k) = \frac{1}{1 - \rho\ c^{(2)}(k)}, \tag{12}$$

with the bulk fluid number density ρ. Once the pair direct correlation function is known, the static structure factor can be calculated directly. Within DFT it is possible to obtain direct correlation functions by functional variation of the excess free energy functional. For the pair direct correlation function one has [49]

$$c^{(2)}(r = |\mathbf{r_1} - \mathbf{r_2}|) = -\beta \frac{\delta^2 \mathcal{F}_{ex}[\rho]}{\delta\rho(\mathbf{r_1})\delta\rho(\mathbf{r_2})}, \tag{13}$$

where $\beta = 1/(k_B T)$.

Employing the structure of FMT for a mixture one finds for the pair direct correlation function for particles of species i and j

$$c_{ij}^{(2)}(r = |\mathbf{r_1} - \mathbf{r_2}|) = -\sum_{\alpha,\gamma} \frac{\partial^2 \Phi_{FMT}}{\partial n_\alpha \partial n_\gamma} \int d\mathbf{r}' \omega_i^\alpha(\mathbf{r}' - \mathbf{r_1}) \omega_j^\gamma(\mathbf{r}' - \mathbf{r_2}). \tag{14}$$

Since we are interested in a bulk fluid, the derivative of Φ_{FMT} w.r.t. weighted densities are functions of the fluid bulk density, but do not depend on location in space. With the help of the convolution theorem the Fourier transform of the pair direct correlation function can be written as

$$c_{ij}^{(2)}(k) = -\sum_{\alpha,\gamma} \frac{\partial^2 \Phi_{FMT}}{\partial n_\alpha \partial n_\gamma}\ \omega_i^\alpha(k)\ \omega_j^\gamma(-k). \tag{15}$$

The second derivatives of Φ_{FMT} w.r.t. the weighted densities and the Fourier transforms of the weight functions are known analytically and hence we arrive at analytical expressions for $c_{ij}^{(2)}(k)$.

For the one-component fluid the analytical expression for the pair direct correlation function as a function of the packing fraction $\phi = (\pi/4)\rho\sigma^2$ is given by

$$\begin{aligned} c^{(2)}(k) = \frac{\pi}{6(1-\phi)^3 k^2} \Bigg\{ & -\frac{5}{4}(1-\phi)^2 k^2 \sigma^2 J_0(k\sigma/2)^2 \\ & + \left(4((\phi - 20)\phi + 7) + \frac{5}{4}(1-\phi)^2 k^2 \sigma^2 \right) J_1(k\sigma/2)^2 \\ & + 2(\phi - 13)(1-\phi) k\sigma J_1(k\sigma/2) J_0(k\sigma/2) \Bigg\}, \end{aligned} \tag{16}$$

where σ is the diameter of the disks and $J_i(x)$ are Bessel functions of the first kind. By inserting this into Eq. (12) we have the structure factor in closed form in the approximation of the FMT functional. The limit of vanishing wave number, Eq. (2), can be taken analytically

$$S(k \to 0) = k_B T \rho \chi_T = \frac{(1-\phi)^3}{1+\phi}, \tag{17}$$

which is consistent with the result from the scaled-particle theory equation of state

[54, 55]

$$\beta p = \frac{\rho}{(1-\phi)^2} \tag{18}$$

that underlies the functional [52] employed here.

For binary mixtures the partial static structure factors are given by [48]

$$S_{ij}(k) = c_i\delta_{ij} + c_i c_j \rho\, h_{ij}(k), \tag{19}$$

where $h_{ij}(k)$ is the total correlation function between particles of species i and j. Note that i and j may either be s or l. For a binary mixture the solution of the Ornstein-Zernike equation takes the form

$$h_{ij}(k) = \frac{N_{ij}(k)}{D(k)}, \tag{20}$$

with a common denominator

$$D(k) = 1 - \rho_s c_{ss}(k) - \rho_l c_{ll}(k) + \rho_s\rho_l \left(c_{ss}(k)c_{ll}(k) - c_{ls}(k)^2\right), \tag{21}$$

where $\rho_{l,s} = c_{l,s}\rho$ are the number densities of the large or small particles. The numerators that depend on the correlation function considered:

$$N_{ss}(k) = c_{ss}(k) - \rho_l \left(c_{ss}(k)c_{ll}(k) - c_{ls}(k)^2\right), \tag{22}$$

$$N_{ll}(k) = c_{ll}(k) - \rho_s \left(c_{ss}(k)c_{ll}(k) - c_{ls}(k)^2\right), \tag{23}$$

and

$$N_{ls}(k) = c_{ls}(k). \tag{24}$$

This is clearly more involved than the corresponding theory for a one-component fluid.

In order to evaluate these expressions the pair direct correlation functions $c_{ij}(k)$ for a mixture are required of particles from species i and j with diameter σ_i and σ_j, respectively. From Eq. (15) we obtain

$$\begin{aligned} c_{ij}(k) = \frac{\pi}{6(1-n_2)^3k^2}\Bigg\{ & \frac{\sigma_i}{2}J_1(k\sigma_i/2)\left[\frac{\sigma_j}{2}\left(5k^2(1-n_2)^2 - 12n_1^2 - 24\pi n_0(1-n_2)\right)J_1(k\sigma_j/2)\right. \\ & \left. - 12k(1-n_2)(\frac{n_1\sigma_j}{2} - n_2 + 1)J_0(k\sigma_j/2)\right] \\ & - (1-n_2)\frac{k\sigma_j}{2}(12J_0(k\sigma_i/2)((1-n_2)\frac{k\sigma_i}{2}J_0(k\sigma_j/2) \\ & + (\frac{n_1\sigma_i}{2} - n_2 + 1)J_1(k\sigma_j/2)) - \frac{7k\sigma_i}{2}(1-n_2)J_2(k\sigma_i/2)J_2(k\sigma_j/2))\Bigg\}, \end{aligned} \tag{25}$$

with the scaled particle variables $n_2 = (\pi/4)(\rho_s\sigma_s^2 + \rho_l\sigma_l^2) = \phi_t$, $n_1 = \pi(\rho_s\sigma_s + \rho_l\sigma_l)$, and $n_0 = \rho_s + \rho_l = \rho$. The pair direct correlation functions and the resulting structure functions are similar in spirit but more consistent than those based on an earlier version of FMT for hard disks due to Rosenfeld [53], where an "approximate

addition theorem" for Bessel functions was employed to correct empirically for missing terms in the excess free energy functional.

As a consistency check we have confirmed that the pair direct correlation function for a mixture, Eq. (25), reduces to the one-component expression, Eq. (16), if either one of the densities is set to zero or the diameters of the mixture are made equal.

3. Experimental methods and data analysis

3.1. *Colloidal model system*

The quasi-2D colloidal hard sphere system studied here was first introduced in [45] and consists of particles confined by gravity to a monolayer on the base of a glass sample cell. In this work, we consider two monodisperse (MD) systems of particles with diameters $\sigma = 2.79$ μm and $\sigma = 4.04$ μm and two binary mixtures: a small size ratio (SSR) system of $\sigma_s = 2.79$ μm and $\sigma_l = 4.04$ μm particles, with $\gamma = \sigma_l/\sigma_s = 1.45$, and a large size ratio (LSR) system of $\sigma_s = 2.79$ μm and $\sigma_l = 6.10$ μm particles, with $\gamma = 2.19$. Systems are considered at a variety of packing fractions, $\phi_i = (\pi/4)\rho_i\sigma_i^2$, where ρ_i and σ_i with $i = l, s$ are the number densities and diameters of the large or small particles, respectively, and the total packing fraction for the system is defined as $\phi_t = \phi_l + \phi_s$. All of the different systems studied are shown in the state diagram in Fig. 1a.

Binary systems are studied at the same constant composition as defined by the number concentration, $c_i = N_i/N$, as it is clear from Eqs. (3) – (5) that c_i governs the effect of composition upon the static structure factors. Note that in Fig. 1(a) this results in groups of points with different gradients for the two binary systems as this plot reflects the packing fraction ratio rather than concentration ratio. This packing fraction ratio is characterised by the parameter $q = \phi_l/\phi_t$, which is equal to 0.37 for the SSR system and 0.48 for the LSR system.

Both binary systems display a non-additivity as the centres of particles of different sizes do not lie in the same plane when sedimented on the base of the glass sample cell, as illustrated in Fig. 1(b) and (c). This is described by the non-additivity parameter Δ, which is defined by [20]

$$\sigma_{ls} = \frac{1}{2}(\sigma_l + \sigma_s)(1 + \Delta), \tag{26}$$

with $\Delta = -0.017$ for the SSR system and $\Delta = -0.070$ for the LSR system. Note that while the two size ratios for the two binary systems do not differ significantly, there is a much greater variation in the non-additivity parameter, though we have shown that the effect of the non-additivity in the SSR system is negligibly small [45]. The negative sign of the non-additivity indicates that the closest distance between unlike particles in the binary system is lower than the sum of their hard disk radii, and thus the particles have a smaller in-plane diameter and thus smaller effective

	σ_l	σ_s	γ	γ'	c_l	Δ
MD	-	2.79	-	-	0	-
MD	4.04	-	-	-	1	-
SSR	4.04	2.79	1.45	1.41	0.215	-0.017
LSR	6.10	2.79	2.19	1.96	0.200	-0.070

Table 1. Parameters for the experimental systems considered, including particle diameters (in μm), the size ratio γ, the effective size ratio γ', the large particle number concentration c_l, and the non-additivity parameter Δ. Note that the number concentration of small particles $c_s = 1 - c_l$.

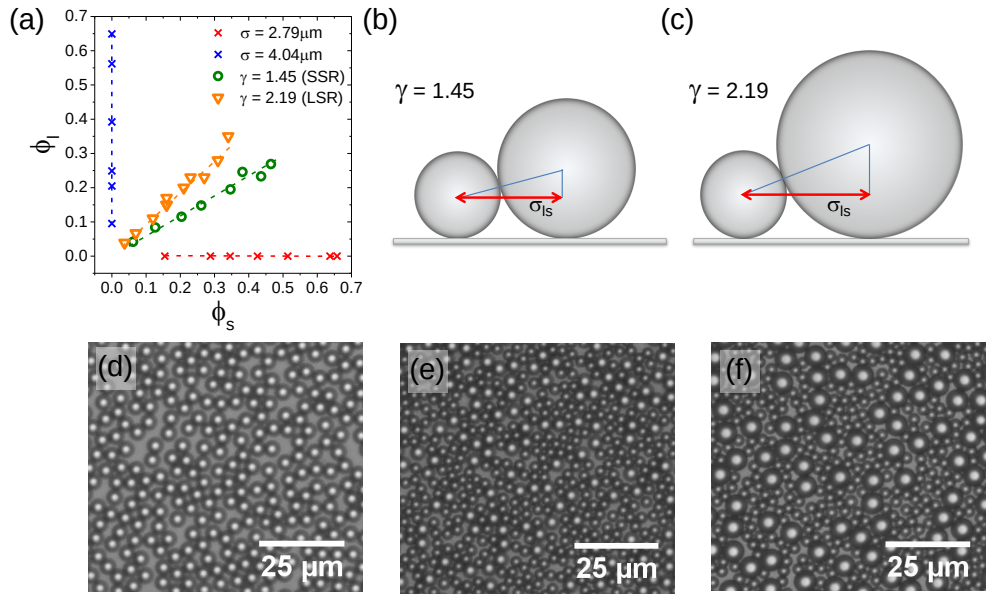

Figure 1. (a) State diagram indicating the different colloidal systems studied. For binary mixtures, those at small size ratio ($\gamma = 1.45$) are represented by green diamonds and those at large size ratio ($\gamma = 2.19$) by orange triangles. Monodisperse systems of particles with diameters of $\sigma = 2.79$ μm and $\sigma = 4.04$ μm are indicated by red and blue crosses, respectively. The in-plane geometry of the (b) small and (c) large size ratio systems. Panels (d) to (f) show experimental images of the (d) monodisperse system with $\sigma =$ 4.04μm (e) small size ratio system ($\gamma = 1.45$) and (f) large size ratio system ($\gamma = 2.19$) at $\phi_t \approx 0.6$.

size ratio, γ'. The difference between the effective radius and the hard disk radius is small for the SSR system, but is more significant at large size ratios and thus for the LSR system effective diameters are used to determine the total packing fraction. A summary of the key parameters for the four experimental systems considered here are given in Table 1.

The colloidal monolayers are imaged using an inverted brightfield video microscope as described in [45, 56]. The images are recorded at 2 frames per second for up to 45 min and particle coordinates obtained using standard routines [57], with typical images of the monodisperse and binary systems shown in Fig. 1(d) to (f).

3.2. *Structure factors*

We calculate the structure factors for monodisperse and binary systems directly from particle positions as

$$S_{ij}(\mathbf{k}) = \frac{1}{N}\left\langle \sum_{\nu=1}^{N_i}\sum_{\mu=1}^{N_j} \cos(\mathbf{k}\cdot\mathbf{r}_\nu)\cos(\mathbf{k}\cdot\mathbf{r}_\mu)\right\rangle + \frac{1}{N}\left\langle \sum_{\nu=1}^{N_i}\sum_{\mu=1}^{N_j} \sin(\mathbf{k}\cdot\mathbf{r}_\nu)\sin(\mathbf{k}\cdot\mathbf{r}_\mu)\right\rangle, \quad (27)$$

which is equivalent to Eq. (1), where $\mathbf{r}_{\nu,\mu}$ is the position of particle ν of species i or μ of species j and $\mathbf{k}$ is the $k-$space vector. As $\mathbf{k}$ is an inverse lengthscale, the magnitude of $\mathbf{k}$ has a minimum value for $k = |\mathbf{k}| = 2\pi/L$, where L is the size of the system as a whole. This minimum value sets the spacing between the vectors in $k-$space such that, in 2D, $\mathbf{k} = 2\pi/L(n_x\hat{\mathbf{x}} + n_y\hat{\mathbf{y}})$, where n_x and n_y are integers

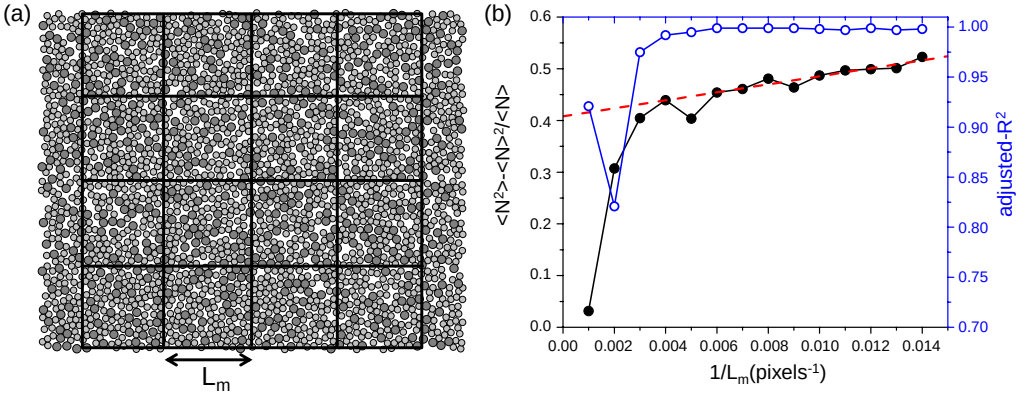

Figure 2. (a) An illustration of splitting particle positions for the sub-box analysis, here with $m = 4$. (b) An example of the extrapolation to infinite system size. Here, the filled symbols show the fluctuations in particle number (Eq. (29)) as a function of box length L_m for one packing fraction and the open symbols indicate the quality of the Gaussian fit to the distribution of values. The dashed line shows the linear fit to the data for $1/L_m > 0.005$ used for the extrapolation.

and $\hat{\mathbf{x}}$ and $\hat{\mathbf{y}}$ are unit vectors in the x and y directions. As the system is isotropic, an azimuthal average over $k-$space vectors of equal magnitude is performed.

3.3. *The $S(k \to 0)$ limit from fluctuations*

The $k \to 0$ limits of the structure factors, which are directly related to thermodynamic quantities, can be obtained by considering fluctuations. For example, for monodisperse systems the $S(k \to 0)$ leads to the isothermal compressibility via Eq. (2), which, in the thermodynamic limit, is directly linked to the fluctuations in the number of particles as [48]

$$S(k \to 0) = \rho k_B T \chi_T = \frac{\langle N^2 \rangle - \langle N \rangle^2}{\langle N \rangle}. \tag{28}$$

For binary systems, the $k \to 0$ limits of the Bhatia–Thornton structure factors are also linked to fluctuations as [1–3]

$$S_{nn}(0) = [\langle N^2 \rangle - \langle N \rangle^2]/\langle N \rangle, \tag{29}$$

$$S_{cc}(0) = N[\langle c_i^2 \rangle - \langle c_i \rangle^2], \tag{30}$$

$$S_{nc}(0) = N[\langle N_i \rangle / \langle N \rangle - \langle c_i \rangle], \tag{31}$$

which allows for an independent measure of the thermodynamic quantities related to these $k \to 0$ limits (see Eqs. (6) – (8)) from a fluctuation analysis.

The fluctuations in Eqs. (28) – (31) are associated with macroscopic fluctuations of the number of particles and the concentration. In a finite system, they can be computed either by an extrapolation of the Bhatia–Thornton structure factors, Eqs. (3) – (5), to $k \to 0$ or by a sub-box analysis [58, 59]. In the latter case, the fluctuations in particle number or concentration in a box with well defined lengthscale, L_m, are computed for the monodisperse systems via Eq. (28) and for the binary systems using Eqs. (29) – (31). In order to determine these expressions in the thermodynamic limit, i.e. for an infinite system the fluctuations are computed as a function of box length for multiple box sizes and extrapolated to infinite box length to determine $S(k) \to 0$. For the experimental images with a frame size of 1280×1024 pixels, a square box with $L = 1000$ pixels positioned in the centre of the

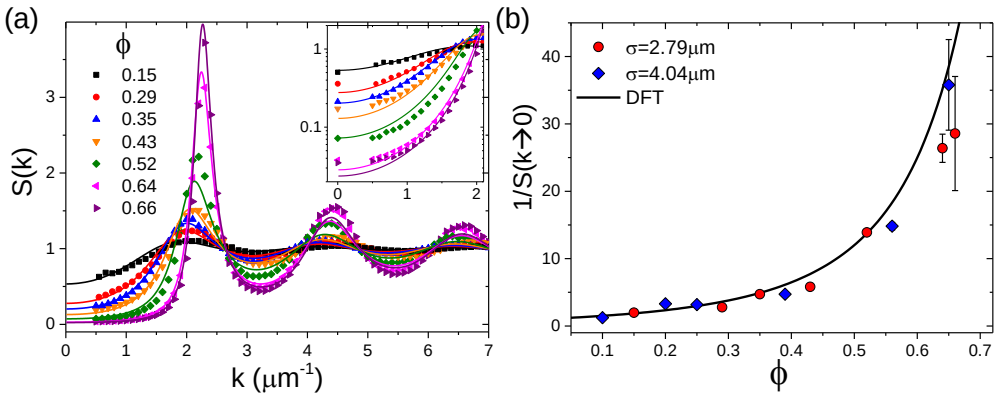

Figure 3. (a) The static structure factors, $S(k)$, for the monodisperse, $\sigma = 2.79$ μm system for a range of packing fractions. The symbols denote data from experiments, while lines correspond to the theoretical structure factor based on Eq. (16). Inset is the small k limit of $S(k)$ for the same system where points at $k = 0$ are those determined by an analysis of number fluctuations. (b) A comparison of the theoretical expression for the $1/S(k \to 0)$ limit (Eq. (17)) with the experimentally determined limit from an analysis of number fluctuations for both monodisperse systems with $\sigma = 2.79$ μm and $\sigma = 4.04$ μm.

frame defines the maximum lengthscale. This area is then split into an $m \times m$ grid of squares, where m runs from 1 to 14, with the side of each square $L_m = 1000/m$ pixels. An example of this for a binary system is shown in Fig. 2(a). Note that as the number of boxes considered increases with decreasing boxsize better statistics are achieved for smaller L_m. Fluctuations in number or concentration of particles for all systems and box lengths are calculated over 500–700 frames, and to ensure that sufficient statistics are achieved for each box size we compare our results to the expected Gaussian form of the distribution. Only results with sufficiently Gaussian number distributions (as quantified by the adjusted R-Square of the fit) are used for the linear extrapolation (see Fig. 2(b)) and the error bars for the $k \to 0$ values in Eqs. (28) – (31) correspond to the errors on the intercept of these linear fits.

4. Results and discussion

4.1. *Monodisperse hard spheres*

First we consider the static structure factor for monodisperse systems. In Fig. 3(a) we show $S(k)$ for the monodisperse system with $\sigma = 2.79$ μm for a variety of packing fractions ϕ as symbols and compare these data to results from the Ornstein-Zernike route to $S(k)$ based on the analytical expression for the pair direct correlation function Eq. (16).

The first peak in $S(k)$ relates to structure on the lengthscale of a particle diameter, σ, with the behaviour at smaller k, reflecting real-space structure which exists over larger length scales. As expected, as ϕ increases, $S(k)$ exhibits a greater degree of structure and a lower value in the limit $k \to 0$, consistent with the greater pressure in the system. The latter is seen more clearly in the inset where we also compare the small k region of $S(k)$ with the results for the $k \to 0$ limit obtained from the sub-box analysis of the number fluctuations (data points at $k = 0$). Good agreement is seen between the apparent limit of the measured $S(k)$ and the limit calculated from number fluctuations by Eq. (28). We also find good agreement between the experimental and the theoretical results, where especially for small values of k – up to the first local minimum – the agreement between theory and experiment is very good without fitting parameters. Successive oscillations in $S(k)$ are less well described by theory than the lower k behaviour and we have confirmed

by standard Monte-Carlo computer simulations [60] that the experimental data match within error bars those for the hard disk structure factors from simulations, while there are clear deviations between the analytical theory and simulations. It is worth pointing out that it would be possible to obtain theoretical predictions for $S(k)$ from a Fourier transform of the radial distribution function $g(r)$ calculated by minimising the FMT functional [45]. While the agreement between theory and experiment along this route is significantly better, we did not follow it here, as the predictions are purely numerical and do not provide additional insight. The same qualitative behaviour is also seen for the monodisperse system with $\sigma = 4.04$ µm.

While the fluctuation analysis appears to provide a good measure of the $k \to 0$ limit of the static structure factors we now verify more fully that this protocol allows for an accurate determination of the isothermal compressibility by considering the equation of state. For our monodisperse systems, this has previously been found to be in excellent agreement with the result from scaled particle theory, Eq. (18) [43, 45], which underlies the FMT functional for hard disks employed here [52]. Therefore in Fig. 3(b) we compare $1/S(k \to 0)$ as computed from Eq. (28) for both monodisperse systems, to the prediction for this quantity based on scaled particle theory, Eq. (17). In general, good agreement between the prediction from SPT and the experimental data is seen, although this deteriorates a little at higher packing fraction. This may be due to insufficient statistics for the higher packing fractions, where a greater length of time is required for the system to fully sample enough different configurations and thus for the analysis to fully capture the behaviour of the fluctuations. Overall, however, the agreement between the experimental results from the fluctuation analysis and theory indicates the validity of this approach to finding the small k limit of $S(k)$.

4.2. *Binary hard spheres*

We next consider the static structure factors for the two different binary mixtures. To this end, in Fig. 4 we plot the three experimental Bhatia–Thornton structure factors for the small (panels (a), (c) and (e)) and large (panels (b), (d) and (f)) size ratio binary systems. In all cases, the degree of structure in the systems increases with increasing total packing fraction. However, clear differences are seen between the structure factors for the LSR and SSR systems. This firstly arises due to the greater disparity in size between the particles at large size ratio, which leads to new peaks appearing in the structure factors, most clearly seen in $S_{nn}(k)$. As $S_{nn}(k)$ is a simple addition of the partial structure factors (Eq. (3)), it is dominated by those partial structure factors linked to the majority component, here the small particles and therefore $S_{ss}(k)$ and $S_{ls}(k)$. For the SSR system, the similarity in size of the different particle species results in similar positions of the initial peaks in $S_{ss}(k)$ and $S_{ls}(k)$. Therefore, the calculated number-number structure factor closely resembles that of the monodisperse system in Fig. 3. In contrast to this, for the LSR the disparity in particle size leads a greater separation in peak positions, resulting in a more complex structure in $S_{nn}(k)$, as illustrated by the apparent splitting of the first peak.

In addition to these obvious particle size effects, however, are differences that result from the different mixing tendencies of the two systems, as quantified by the structure factors that consider concentration fluctuations, $S_{cc}(k)$ and $S_{nc}(k)$. In both SSR and LSR mixtures, the negative non-additivity, Δ, makes it favourable for there to be more contacts between unlike particles as this reduces the effective particle diameters and thus increases the free area. In spite of this, it has previously been shown that the equilibrium structure of the SSR system is in excellent agree-

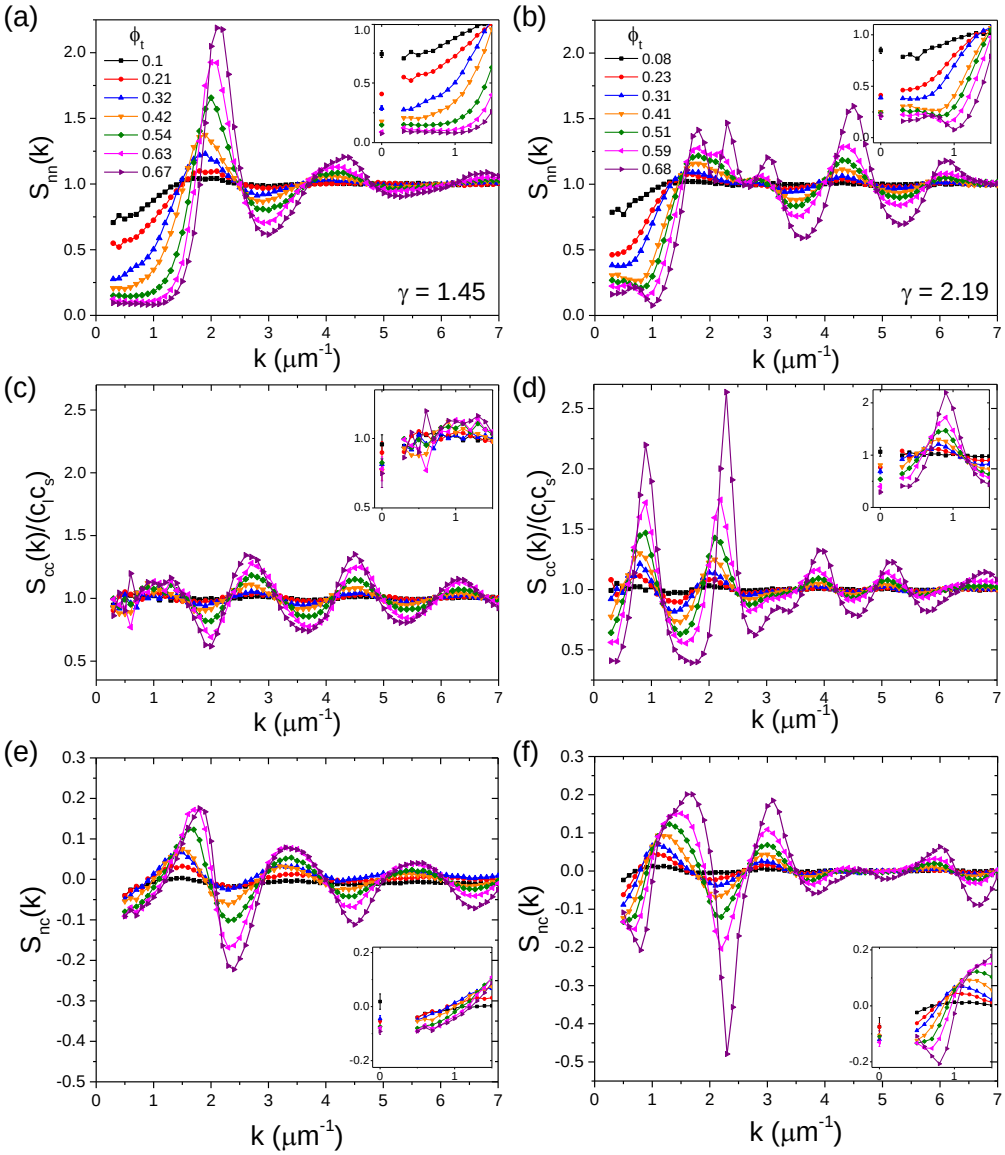

Figure 4. The experimental Bhatia–Thornton structure factors, shown as symbols with connecting lines, for the binary colloidal systems at two size ratios: (a) and (b) the number-number structure factor, $S_{nn}(k)$ for the SSR and LSR systems respectively; (c) and (d) the concentration-concentration structure factor, $S_{cc}(k)$ for the SSR and LSR systems respectively; and (e) and (f) the number-concentration structure factor, $S_{nc}(k)$ for the SSR and LSR systems respectively. The insets show a zoom of the corresponding structure factors at small k and the $k \to 0$ limits calculated from the box size analysis of fluctuations in number or concentration of particles. Note that the packing fractions in (c) and (e) are as shown in (a), whilst packing fractions in (d) and (f) are as those in (b).

ment with that predicted for additive binary mixtures from fundamental measure theory [45], showing that here the small non-additivity has little effect. For the LSR system, however, Δ is almost four times larger than for the SSR system and so the drive towards mixing is clearly more significant, and this is reflected in the more pronounced peaks in $S_{cc}(k)$ and $S_{nc}(k)$. Furthermore, the tendency towards mixing in the LSR system results in a suppression of concentration fluctuations, which is clearly seen in the drop of the small k limit of $S_{cc}(k)$ with increasing ϕ_t (Fig. 4(d)). The presence of structure on a larger scale is also indicated by the peak in $S_{nn}(k)$ as $k \to 0$ for the LSR system at $\phi_t = 0.68$ (Fig. 4(b)), which is absent in the corresponding SSR structure factor (Fig. 3(a)).

A direct comparison between the experimental and theoretical structure factors

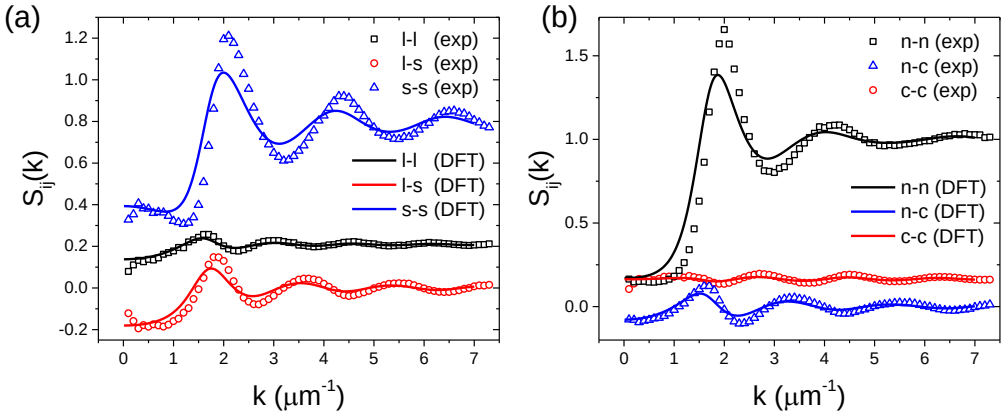

Figure 5. (a) A comparison between theory (lines) and experiments (symbols) of the partial structure factors $S_{ss}(k)$, $S_{ls}(k)$, and $S_{ll}(k)$ for the SSR with $\phi_t = 0.54$. The results agree qualitatively, however, due to the high concentration of the small disks there are clear deviations between theory and experiments found in $S_{ss}(k)$. This deviation can also be found in the Bhatia–Thornton structure factors, shown in (b), where in particular $S_{nn}(k)$ shows discrepancies.

is more challenging in the case of mixtures. In fact, as the theory is based on an FMT functional for *additive* hard-disk mixture, we only compare the theory to the experimental structure factors for the SSR system, where the effect of the non-additivity is negligible [45]. Note that such comparison is not meaningful for the LSR system due to the significant non-additivity. We show an example for the SSR system with $\phi_t = 0.54$ in Fig. 5, where we plot both the partial structure factors $S_{ij}(k)$ in (a) and the Bhatia–Thornton linear combinations in (b). Due to the large concentration of small disks $S_{ss}(k)$ clearly dominates the structure of the mixture. Qualitatively this is captured by the theory, even though the extension of the Ornstein-Zernike equation from a one-component fluid to a binary mixture introduces much more complexity. The agreement between theory and experiment for $S_{ll}(k)$ and $S_{ls}(k)$ for the parameters used here is significantly better than for $S_{ss}(k)$, as can be seen in Fig. 5(a), which is due to the fact that the SSR system is rich in small particles. Furthermore, the level of agreement is better for smaller values of ϕ_t, while it becomes worse as ϕ_t is further increased, as at higher ϕ_t the errors in the (complex) direct pair correlation functions (Eq. (25)) will be more significant, which, in turn, will lead to larger deviations in the structure factors.

It is clear from the deviations between theory and experiments found in $S_{ss}(k)$ that linear combinations of the partial structure factors pick up similar deviations. In Fig. 5(b) we show the Bhatia–Thornton structure factors for SSR with $\phi_t = 0.54$ and find that in particular the $S_{nn}(k)$ exposes the shortcomings of the (analytical) theory. While the qualitative behaviour is reproduced by the theory, the level of agreement is far from being quantitative. The $S_{nc}(k)$ and $S_{cc}(k)$ from theory again agree on a better level with the corresponding experimental data.

We now consider the $k \to 0$ limit of the experimental Bhatia–Thornton structure factors in more detail – note that a detailed analysis of the theoretical structure factors at $k \to 0$ was not pursued at this stage given the lack of quantitative agreement. The small k regions of $S_{nn}(k)$, $S_{cc}(k)$ and $S_{nc}(k)$ are again shown as insets in Fig. 4 with the points at $k = 0$ computed using the relevant fluctuation analysis for each structure factor from Eqs. (29) – (31). In all cases the fluctuation analysis is in good agreement with the $k \to 0$ limit of the structure factors suggesting that this provides a good estimate of the corresponding thermodynamic quantities. Importantly, the fluctuation analysis allows for the limits of all three Bhatia–Thornton structure factors to be obtained independently.

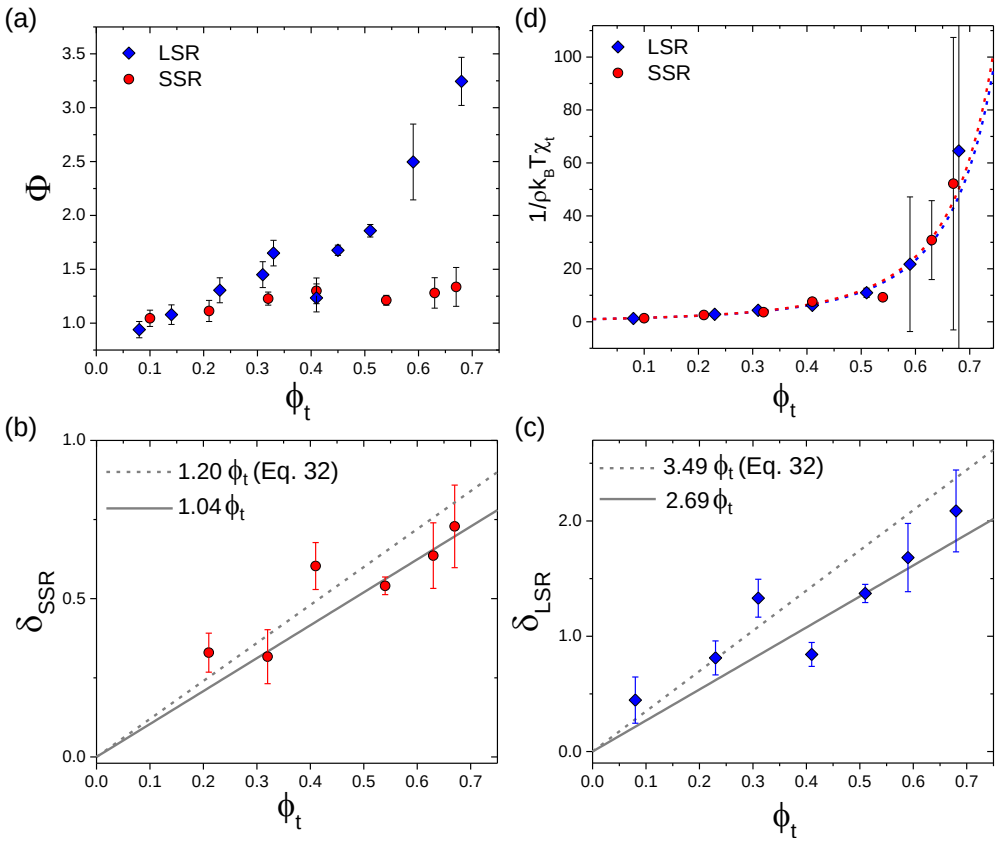

Figure 6. (a) The thermodynamic factor Φ as a function of total packing fraction ϕ_t for both binary colloidal fluids. (b, c) The dilatation factors δ as a function of total packing fraction for the small size ratio (b) and large size ratio (c) systems. Solid grey lines show the linear fit to the data used to approximate δ and dashed grey lines show the prediction from Eq. (32). Error bars are the combined errors from $S_{nc}(0)$ and $S_{cc}(0)$ (see Eq. (8)). (d) The isothermal compressibility expressed as $1/\rho k_B T \chi_T$ for the colloidal binary systems at large and small size ratio as a function of ϕ_t. Blue and red dashed lines show the prediction for the equation of state from scaled particle theory [55]. Error bars are the combined errors from $S_{nn}(0)$, $S_{nc}(0)$ and $S_{cc}(0)$ (see Eq. (6)). Note that the error bar for the data point for the LSR system at $\phi_t = 0.68$ is larger than the range of the axis.

The simplest thermodynamic quantity to extract is the thermodynamic factor, Φ, as this is computed from the limit of $S_{cc}(k)$ alone, using Eq. (7). Importantly, Φ acts as a quantitative measure of the degree to which the system displays mixing effects, and as such Φ has a central role in theories of mutual or interdiffusion [4, 6]. The thermodynamic factor as a function of ϕ_t is plotted in Fig. 6(a) for both the LSR and SSR systems. For the SSR system, only a very small increase in Φ is seen for the packing fractions considered, indicating that the system behaves as an additive hard sphere mixture, in agreement with [45]. In contrast to this, for the LSR system there is a substantial increase in Φ with increasing ϕ_t in accordance with the qualitative behaviour of $S_{cc}(k)$ in Fig. 4(d). This is similar to the behaviour seen in metallic alloys which display chemical short range ordering [6], however for our hard disk model systems, the effect here is entropic in origin.

The second thermodynamic quantity that may be obtained is the dilatation factor, δ, which describes the relationship between system size and composition [1–3]. The experimental dilatation factors – determined via Eq. (8) – for the LSR and SSR systems are plotted in Fig. 6(b) and (c) and exhibit a linear dependence on ϕ_t for both size ratios, though with a steeper gradient for the LSR system. Also shown are linear fits to the data (solid grey lines) from which we find $\delta_{\mathrm{SSR}} = 1.04\phi_t$ and $\delta_{\mathrm{LSR}} = 2.69\phi_t$. To explain the observed linear dependence of δ on ϕ_t, we write – in analogy to its definition for a three-dimensional molecular mixture,

$\delta = \rho(v_1 - v_2)$ [1–3, 48] – the dilatation factor for our colloidal binary monolayers as $\delta = N/A(a_l - a_s)$. Here, the total area of the system is $A = A_0 + N_l a_l + N_s a_s$, with a_i the area of a particle of species i and A_0 the 'unoccupied' area between the particles. Rewriting δ in terms of $q = \phi_l/\phi_t$, $c_l = N_l/N$ and the in-plane size ratio γ' leads to the following expression:

$$\delta = \phi_t \frac{q}{c_l \gamma'}(\gamma'^2 - 1), \tag{32}$$

which indeed shows that δ is directly proportional to ϕ_t and that the slope depends on the size ratio. Using the values for q and c_l for both systems (see Table 1), we can calculate $\delta(\phi_t)$ from Eq. (32) as $\delta_{\mathrm{SSR}} = 1.20\phi_t$ and $\delta_{\mathrm{LSR}} = 3.49\phi_t$, which are shown as dashed grey lines in Fig. 6(b) and (c). For both the SSR and LSR systems, Eq. (32) slightly overestimates the gradient, but the agreement is still remarkable given the fact that there are no fitting parameters.

Finally, having established the values of $S_{cc}(0)$ and expressions for δ these can be combined with $S_{nn}(0)$ using Eq. (6) to determine the isothermal compressibility χ_T as a function of ϕ_t, which is shown for both binary mixtures in Fig. 6(d). Note that towards high ϕ_t the error bars become relatively large, which underlines the difficulty in obtaining the isothermal compressibility for binary fluids at high packing fractions. This is due to the error in χ_T being the combined errors from $S_{nn}(0)$, $S_{nc}(0)$ and $S_{cc}(0)$ (see Eq. (6)) and $\rho k_B T \chi_T$ becoming very small as $1/(\rho k_B T \chi_T)$ diverges at high packing fractions. As with the monodisperse system, we compare these results to the prediction from scaled particle theory for binary mixtures [55]. In both cases, good agreement is seen with the theoretical expression over the full range of fluid packing fractions, with very similar values of the isothermal compressibility found for the two binary systems. This implies that measurement of the isothermal compressibility does not distinguish between the two binary systems in spite of their quite different structures. As such, whilst for a monodisperse system determining a single equation of state in terms of the isothermal compressibility is sufficient, for binary mixtures a full understanding of the thermodynamics of the system requires the measurement of multiple 'equations of state' that capture the effects of both particle number and concentration fluctuations.

5. Conclusion

In conclusion, we have performed a detailed analysis of the static structure factors of monodisperse fluids and two binary colloidal hard sphere mixtures with size ratios of $\gamma = 1.45$ and $\gamma = 2.19$ in two dimensions. We have compared data from detailed experiments for the monodisperse fluids and the small size ratio binary system to theoretical predictions based on the Ornstein-Zernike route employing analytical pair direct correlation functions derived from a recent FMT functional for additive hard-disk mixtures [52]. We find good agreement between theory and experiments for the monodisperse case, while qualitative agreement is found for the small size ratio binary system, for which the non-additivity in the experiments is negligible [45], but the theory is much more complex.

In particular, for the colloidal binary fluids, we have calculated the Bhatia–Thornton structure factors from the partial static structure factors. We have also determined the short wavevector ($k \to 0$) limits of the structure factors directly and from an analysis of number and concentration fluctuations, which leads to the equations of state for the systems. For monodisperse and binary systems the isothermal compressibility as a function of total packing fraction is found to be well

described by results from scaled particle theory, with very little difference found between the isothermal compressibilities for the two binary systems. In contrast, the thermodynamic factor as a function of the total packing fraction is found to depend strongly on the size ratio, which we ascribe to differences in the mixing tendencies of the two systems due to their differing negative non-additivities, which is negligible in the small size ratio system [45], but significant in the large size system.

Acknowledgements

We thank Daan Frenkel and Bob Evans for numerous useful discussions. The EPSRC, Royal Society and ERC (ERC Starting Grant No. 279541-IMCOLMAT) are acknowledged for financial support.

Data availability

The data that support the findings of this study are available from the corresponding author, RPAD, upon reasonable request.

References

[1] A.B. Bhatia and D.E. Thornton, Phys. Rev. B **2** (8), 3004 (1970).
[2] A.B. Bhatia, W.H. Hargrove and D.E. Thornton, Phys. Rev. B **9** (2), 435 (1974).
[3] A.B. Bhatia, Inst. Phys. Conf. Ser. No. 30 p. 21 (1977).
[4] P. Kuhn, J. Horbach, F. Kargl, A. Meyer and T. Voigtmann, Phys. Rev. B **90** (2), 024309 (2014).
[5] F. Faupel, W. Frank, M.P. Macht, H. Mehrer, K. Rätzke, H. Schober, S.K. Sharma and H. Teichler, Rev. Mod. Phys. **75**, 237 (2003).
[6] J. Horbach, S. Das, a. Griesche, M.P. Macht, G. Frohberg and a. Meyer, Phys. Rev. B **75** (17), 174304 (2007).
[7] K. Binder, in *Theories and Mechanism of Phase Transitions, Heterophase Polymerizations, Homopolymerization, Addition Polymerization* (Springer Berlin Heidelberg, Berlin, Heidelberg, 1994), pp. 181–299.
[8] J.W. Barlow and D.R. Paul, Polym. Eng. Sci. **21** (15), 985 (1981).
[9] G. Yatsenko, E.J. Sambriski and M.G. Guenza, J. Chem. Phys. **122** (5) (2005).
[10] K. Binder and W. Kob, *Glassy materials and disordered solids* (World Scientific Pub Co Pte Ltd, Singapore, 2011).
[11] T. Narumi, S.V. Franklin, K.W. Desmond, M. Tokuyama and E.R. Weeks, Soft Matter **7** 1472 (2011).
[12] H. König, R. Hund, K. Zahn and G. Maret, Eur. Phys. J. E **18** (3), 287 (2005).
[13] S. Williams and W. van Megen, Phys. Rev. E **64** (4), 041502 (2001).
[14] G. Foffi, W. Götze, F. Sciortino, P. Tartaglia and T. Voigtmann, Phys. Rev. Lett. **91** (8), 085701 (2003).
[15] S. Amore, J. Horbach and I. Egry, J. Chem. Phys. **134** (4), 044515 (2011).
[16] J. Russo and N.B. Wilding, Phys. Rev. Lett. **119** 115702 (2017).
[17] W. Götze and T. Voigtmann, Phys. Rev. E **67** (2), 021502 (2003).
[18] P. Hopkins and M. Schmidt, J. Phys.: Condens. Matter **22** 325108 (2010).
[19] T. Biben, P. Bladon and D. Frenkel, J. Phys.: Condens. Matter **8** (50), 10799 (1996).
[20] R. Roth, R. Evans and A.A. Louis, Phys. Rev. E **64**, 051202 (2001).
[21] M. Rovere and G. Pastore, J. Phys.: Condens. Matter **6**, A163 (1994).
[22] S.K. Das, J. Horbach, K. Binder, M.E. Fisher and J.V. Sengers, J. Chem. Phys. **125** (2), 24506 (2006).
[23] K. Jagannathan and A. Yethiraj, J. Chem. Phys. **118** (17), 7907 (2003).
[24] A. Imhof and J.K. Dhont, Phys. Rev. Lett. **75** (8), 1662–1665 (1995).
[25] D.J. Ashton, J. Liu, E. Luijten and N.B. Wilding, J. Chem. Phys. **133** (19), 194102 (2010).
[26] F. Lo Verso, D. Pini and L. Reatto, J. Phys.:Condens. Matter **17** (6), 771–796 (2005).
[27] T. Kawasaki and H. Tanaka, J. Phys. Condens. Matter **23** (19), 194121 (2011).
[28] J.M. Lynch, G.C. Cianci and E.R. Weeks, Phys. Rev. E **78** (3), 1–7 (2008).
[29] P. Bartlett, J. Phys.: Condens. Matter **2** (22), 4979 (1990).
[30] C.P. Royall, E.C.M. Vermolen, A. Van Blaaderen and H. Tanaka, J. Phys.: Condens. Matter **20** (40) (2008).
[31] F.A. Lavergne, S. Diana, D.G.A.L. Aarts and R.P.A. Dullens, Langmuir **32** 12716 (2016).
[32] C. Grodon, M. Dijkstra, R. Evans and R. Roth, J. Chem. Phys. **121** (16), 7869 (2004).
[33] C. Grodon, M. Dijkstra, R. Evans and R. Roth, Mol. Phys. **103** (21-23), 3009–3023 (2005).
[34] J. Baumgartl, R.P.A. Dullens, M. Dijkstra, R. Roth and C. Bechinger, Phys. Rev. Lett. **98** (19), 198303 (2007).
[35] A. Statt, R. Pinchaipat, F. Turci, R. Evans and C.P. Royall, J. Chem. Phys. **144** (14), 144506 (2016).

[36] A.M. Smith, A.A. Lee and S. Perkin, Phy. Rev. Lett. **118** (9), 1–5 (2017).
[37] A. Santos, M. López De Haro and S.B. Yuste, J. Chem. Phys. **122** (2) (2005).
[38] M. Schmidt, J. Phys.: Condens. Matter **16**, L351 (2004).
[39] P. Pusey and W.V. Megen, Nature **320** (27), 340–342 (1986).
[40] E.P. Bernard and W. Krauth, Phys. Rev. Lett. **107** (15), 155704 (2011).
[41] M. Engel, J.A. Anderson, S.C. Glotzer, M. Isobe, E.P. Bernard and W. Krauth, Phys. Rev. E **87** (4), 042134 (2013).
[42] W. Qi, A.P. Gantapara and M. Dijkstra, Soft Matter **10** (30), 5449–57 (2014).
[43] A.L. Thorneywork, J.L. Abbott, D.G.A.L. Aarts and R.P.A. Dullens, Phys. Rev. Lett. **118**, 158001 (2017).
[44] A.L. Thorneywork, J.L. Abbott, D.G.A.L. Aarts, P. Keim and R.P.A. Dullens, J. Phys.: Condens. Matter **30**, 104003 (2018).
[45] A.L. Thorneywork, R. Roth, D.G.A.L. Aarts and R.P.A. Dullens, J. Chem. Phys. **140** (16), 161106 (2014).
[46] A.L. Thorneywork, R.E. Rozas, R.P.A. Dullens and J. Horbach, Phys. Rev. Lett. **115**, 268301 (2015).
[47] D. Stopper, A.L. Thorneywork, R.P.A. Dullens and R. Roth, J. Chem. Phys. **148**, 104501 (2018).
[48] J. Hansen and I. Macdonald, *Theory of Simple Liquids*, 3rd ed. (Academic Press, London, 2006).
[49] R. Evans, Adv. Phys. **28** (2), 143–200 (1979).
[50] Y. Rosenfeld, Phys. Rev. Lett. **63** (9), 980 (1989).
[51] R. Roth, J. Phys. Condens. matter **22** (6), 063102 (2010).
[52] R. Roth, K. Mecke and M. Oettel, J. Chem. Phys. **136** (8), 081101 (2012).
[53] Y. Rosenfeld, Phys Rev A **42**, 5978–5989 (1990).
[54] E. Helfand, H.L. Frisch and J.L. Lebowitz, J. Chem. Phys. **34** (3), 1037 (1961).
[55] J.L. Lebowitz, E. Helfand and E. Praestgaard, J. Chem. Phys. **43** (3), 774 (1965).
[56] A.L. Thorneywork, D.G.A.L. Aarts, J. Horbach and R.P.A. Dullens, Phys. Rev. E **95**, 012614 (2017).
[57] J. Crocker and D. Grier, J. Colloid Interface Sci. **179**, 298 (1996).
[58] M. Rovere, D. Heermann and K. Binder, J. Phys. Condens. Matter **2**, 7009 (1990).
[59] M. Rovere, D. Hermann and K. Binder, Eur. Lett. **6**, 585 (1988).
[60] D. Frenkel and B. Smit, *Understanding Molecular Simulation*, (Elesvier, Amsterdam, 2nd edition, 2002).